University
of Pardubice
Faculty
of Chemical Technology

Investigation of an amphoteric behaviour of arsenic dopant in polycrystalline SnSe

Jiří Navrátil[1]*, Kateřina Šraitrová[2], Vladimír Kucek[2],
Tomáš Plecháček[3], Jana Kašparová[1], and Čestmír Drašar[1]

[1]*Institute of Applied Physics and Mathematics,*
The University of Pardubice, CZ–532 10 Pardubice, Czech Republic

[2]*Department of General and Inorganic Chemistry,*
The University of Pardubice, CZ–532 10 Pardubice, Czech Republic

[3]*Joint Laboratory of Solid State Chemistry,*
The University of Pardubice, CZ–532 10 Pardubice, Czech Republic

We investigated eventual amphoteric behaviour of As atoms in SnSe by substituting in either cation or anion site. The investigation involved two series of polycrystalline samples of nominal composition $Sn_{1-x}As_xSe$ ($0 \leq x \leq 0.1$) and $SnAs_xSe_{1-x}$ ($0 \leq x \leq 0.08$). The prepared powders were identified by X-ray diffraction. Hot-pressed from powder, polycrystalline pellets were used for characterization of transport and thermoelectric properties in temperature range of 300–730 K. An embedding of the As atoms in either cation or anion site seems to prevent formation of the major defects present in the undoped SnSe, tin vacancies V_{Sn}^{2-}. Instead, selenium vacancies V_{Se}^{2+} together with substitutional defects As_{Sn}^+ play the major role in the electronic transport in the $Sn_{1-x}As_xSe$ system. Due to rather low solubility of arsenic in the system ($x \leq 0.02$), either As inclusions or amorphous As-Se phase is formed in highly doped samples. In the case of $SnAs_xSe_{1-x}$, As atoms enter Se position forming As_{Se}^-, which increases the hole concentration in the doped samples at lower temperatures. At higher temperatures, the properties of the compounds (for $x \geq 0.03$) are influenced by the formation of highly conductive AsSn phase. Generally, the substitution of As for both anion and cation lead to no evident enhancement of the thermoelectric figure of merit ZT.

---

* Corresponding author, ✉ Jiri.Navratil@upce.cz

Introduction

The instant growth of global energy demands calls for alternative sources of energy, especially those of a renewable nature. One of such sources which is hard to be ignored is a tremendous amount of waste heat generated by various industrial processes and other human activities. Thermoelectric generation technology represents one of the promising options that is assumed to play an important role in harvesting of the waste heat. Currently, there are a few obstacles for the technology harnessing. Namely, it is rather low conversion efficiency and quite high economic costs that restrict any extensive commercial applications of the individual technologies. The efficiency of these thermoelectric devices can be expressed in terms of figure of merit ZT ($ZT = \sigma \times S^2 \times T/\kappa$, where σ, S, κ, and T are the electrical conductivity, the Seebeck coefficient, the thermal conductivity, and the absolute temperature, respectively) of the materials used for their construction. The potential of an implementation of the thermoelectric technology in waste heat conversion is often expressed in the price per watt (e.g. \$ W^{-1}) term. Thus, the cost of thermoelectric materials, representing an appreciable part of the price of the thermoelectric devices, is one of very important factors in considerations about implementation of the technology. That is why the effort of many researchers in the field turn their attention to the quest for synthesis of new materials composed of nontoxic and earth abundant elements.

Simple binary compounds of the SnSe type (orthorhombic space group *Pnma*) have been surprisingly ignored over years by the thermoelectric community until a report in 2014 [1] which pointed out an unprecedented ZT value (2.6 ± 0.3 at 923 K) for SnSe single crystals measured along the *b*-axis, mainly, due to a very low thermal conductivity in the direction. The compound also fully meets the criterion of an economical availability of raw elements which the compound consists of. Unfortunately, poor mechanical properties of the layered crystals due to an easy cleavability together with a high cost of single-crystals growth prevent their implementation in wider practical applications. That is why the researchers have focused on the study of the compounds in the polycrystalline form. A number of studies have dealt with polycrystalline SnSe compounds doped with various dopants like Ag [2], Cu or In [3], alkaline ions [4–6] and/or their composites with some nano-inclusions [7].

Here, we report on the synthesis and subsequent investigation of the thermoelectric properties of samples of polycrystalline SnSe doped by arsenic. In the study we investigated the eventual amphoteric nature of As in SnSe, i.e. either this element is substituted for Sn ($Sn_{1-x}As_xSe$) or for Se ($SnAs_xSe_{1-x}$).

Materials and methods

Polycrystalline samples with the composition $Sn_{1-x}As_xSe$ and nominal values x between 0 and 0.1 and $SnSe_{1-x}As_x$ with x between 0 and 0.08 were prepared utilizing high temperature reactions. Polycrystalline samples were synthesized from a mixture of pure elements and compounds, Sn (5N shots), AsSn (synthesized), Se (5N shots) that were all obtained from Sigma-Aldrich. The synthesis of AsSn was performed by heating the stoichiometric mixtures of 5N Sn and As (three-times sublimed) to 933 K for 14 days in evacuated ($\approx 10^{-3}$ Pa) quartz ampoules. This material was powdered and mixed with Sn and Se in the ratio corresponding to the stoichiometry $Sn_{1-x}As_xSe$ (x = 0, 0.0025, 0.005, 0.01, 0.02, 0.05 and 0.1) and $SnSe_{1-x}As_x$ to the stoichiometry (x = 0, 0.0015, 0.0025, 0.0035, 0.005, 0.0075, 0.01, 0.02, 0.03, 0.04, 0.06 and 0.08). The synthesis of the polycrystalline products was performed in evacuated, sealed quartz ampoules. These were heated to 1223 K over 10 hours maintained at this temperature for 6 hours, and then cooled down to room temperature by switching off the furnace. The products were powdered for 1 min in a vibrating mill under hexane and identified by X-ray diffraction (XRD). The samples for physical measurements were hot-pressed at 713 K and 70 MPa for 1 hour. Compact disc-shaped samples (with diameter 12 mm and thickness cca 2 mm) and rectangular samples (with dimensions $10 \times 3.5 \times 10$ mm³ and 10 mm in the direction of pressing) reached ≥95 % of theoretical (X-ray) densities of the prepared compounds. Electrical conductivity σ was measured in the 300–725 K temperature range with four-probe method using lock-in amplifier (model 5209; EG&C, Princeton; USA).

The Seebeck coefficient S was determined by means of a static dc method on disc-shaped samples. The temperature gradient between two points was measured with two shielded K-type thermocouples pressed against the sample surface. A potential difference dU corresponding to the gradient dT was measured across the same legs of both attached thermocouples. The absolute Seebeck coefficient was determined from the slope dU/dT.

The thermal diffusivity k was measured from 300 to 725 K on round hot-pressed samples using the respective instrument (model LFA 457; Netzsch-Gerätebau, Selb, Germany). The thermal conductivity κ was subsequently calculated using the relation: $\kappa = k \times c_p \times \rho$, where ρ is the experimental density and c_p the heat capacity. Inconel was used as the heat capacity standard. As the experimental values of the heat capacity c_p could be scattered with the temperature T and composition x (c_p = 0.24–0.34 J g⁻¹ K⁻¹ (Dulong Petit law gives c_V = 0.252 J g⁻¹ K⁻¹)), we used an average c_p = f(T) based on c_p-measurements of all the samples of the $Sn_{1-x}As_xSe$ and $SnSe_{1-x}As_x$ series. We assume that rather low content of As in the host compound has only a negligible effect on the heat capacity of host matrix.

The diffraction patterns (Cu K_α, $\lambda = 1.5418$ Å) were recorded on powdered samples using a diffractometer (model D8 Advance; Bruker AXS, Germany) equipped with a Bragg-Brentano $\varTheta-\varTheta$ goniometer (with radius 217.5 mm), a secondary-beam curved graphite monochromator, and a Na(Tl)I scintillation detector. The scan was performed at room temperature from 10 to 80° ($2\,\varTheta$) in steps of 0.02° with a counting time of 8 s per step. The lattice parameters were refined by the LeBail method within the FullProf program.

μ-XRF spectrometer (model M4 Tornado; Bruker) was then used for composition analysis. The excitation of X-ray fluorescence radiation was performed by a Rh-side window X-ray tube with polycapillary lens offering a spot size down to 25 μm combined with high excitation intensity. Detection of fluorescence radiation was performed by an energy-dispersive silicon drift detector with 30 mm^2 sensitive area and energy resolution of 142 eV for Mn-K_α. The X-ray tube was operated at 50 kV and 200 μA. Analyses were carried out under 20 mbar vacuum conditions and the spectra evaluated using Esprit software (Bruker).

Results and discussion

The XRD patterns collected on the synthesized powders before the hot-pressing process could be fully indexed within the space group *Pnma* of SnSe (JCPDS #48-1224). A small amount of the secondary phases was identified at samples with higher nominal content of As. At the samples of $Sn_{1-x}As_xSe$, the traces of elemental As (JCPDS #07-2052) were detected for $x \geq 0.05$. At the samples of nominal composition $SnAs_xSe_{1-x}$, a cubic compound (*Fm-3m*) of AsSn (JCPDS #04-7507) was observed for x as low as 0.03. Although no other phases have been detected in the powdered samples, it is known from literature that traces of elemental Sn are present in the SnSe compounds [8]. We detected a small broad peak of the elemental tin (JCPDS #13-6165) in the hot-pressed pellets made of the powders (see Fig. 1 and the corresponding inset). Because the pellets were compacted at lower temperatures (713 K) compared to the synthesis temperature, we assume that free tin atoms, present most likely in the freshly synthesized SnSe, aggregate during the hot-pressing process into larger structures as noticed also in ref. [6]. From Fig. 1, there is also evident considerable enhancement of the preferential orientation of the SnSe crystallites along *bc*-planes (the increase of 400 lines) positioned perpendicularly to the pressure direction.
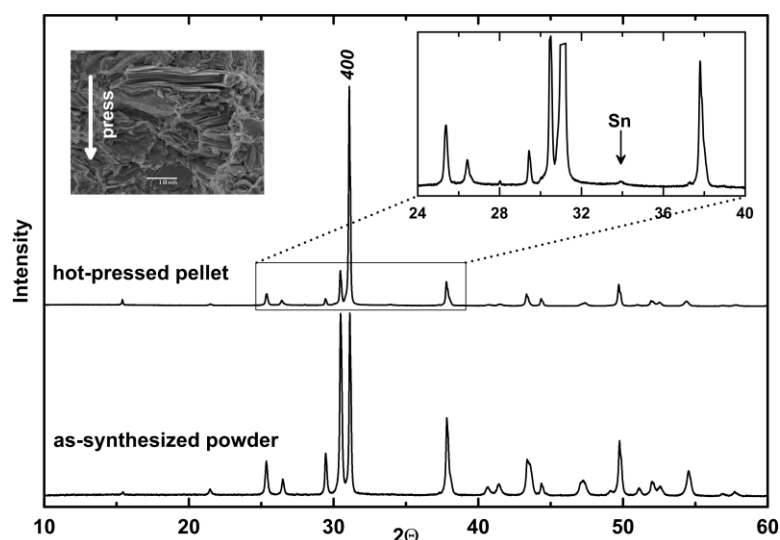
Fig. 1 *XRD patterns of as-synthesized powder of the undoped SnSe sample and the corresponding pellet that were hot-pressed at 713 K and 70 MPa for 1 hr*

The magnified inset (top right) shows the occurrence of elemental Sn (JCPDS #13-6165) in the matrix after the hot-pressing process. The inset (top left) depicts SEM image illustrating a preferential orientation of SnSe crystallites in the prepared pellets.

Fig. 2a displays the variation of unit-cell volume of $Sn_{1-x}As_xSe$ compound with x. All three lattice parameters (a, b, c) vary in the same manner, i.e. they slightly decrease down to about $x \leq 0.02$ and stay nearly constant at higher x values. This decrease of the parameters corresponds to quite profound difference between the ionic radii of Sn^{2+} (118 pm) and As^{3+} (58 pm) [9]. Such a difference also explains the limited solubility of As in SnSe when being substituted for Sn atoms. As mentioned above, the traces of metallic As were observed in samples with higher x in the X-ray patterns and in XRF maps that had also revealed clusters of As (see inset in Fig. 2a). Although the As provides an inhomogeneous embedding in the SnSe structure (inset in Fig. 2a), the XRD patterns do not reveal any corresponding foreign phase in a noticeable concentration. We conclude that the As atoms may form an amorphous As-Se phase that is hard to observe in the XRD patterns. Less likely, an As-rich phase (structure) is formed keeping the structure of the hosting compound SnSe. Maybe this phase enters the hosting structure in epitaxy-like way.

We observed qualitatively similar behaviour of the lattice parameters also for the doping in anion sub-lattice, i.e. when the As atoms substitutes for Se atoms in the $SnAs_xSe_{1-x}$ system. A similarity in the ionic radii of As^{3-} and Se^{2-} ions (222 ppm *vs.* 198 ppm) can be explained by rather constant unit-cell volume (and all the lattice parameters) in low nominal concentrations ($x \leq 0.02$) of As (see Fig. 2b). The formation of AsSn compound observed at higher nominal contents of As in $SnAs_xSe_{1-x}$ suggests us that either a part of As substitutes part of Sn and the Se atoms in the studied compositions or the decrease observed for the lattice

parameters is due to an increase of the Sn deficiency as reported in ref. [10]. The constant and lower values of the unit-cell volumes at higher x (namely: $x \geq 0.03$) indicate a limited solubility of As in $SnAs_xSe_{1-x}$ samples.

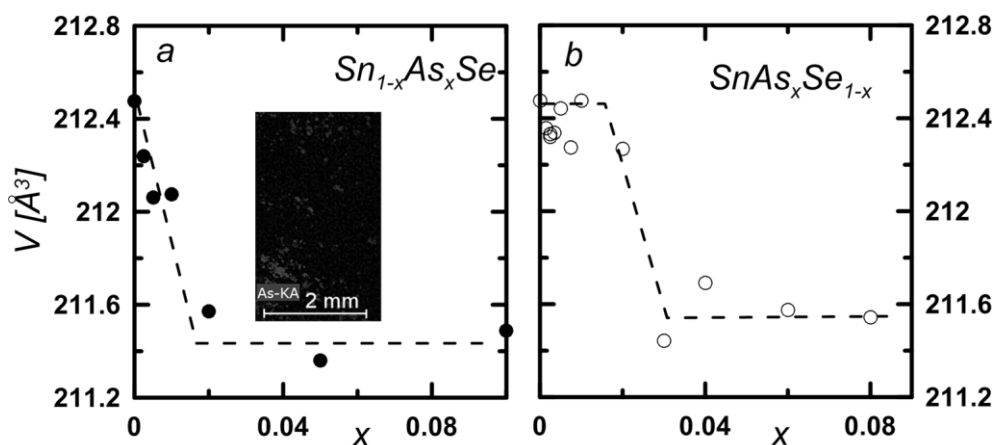**Fig. 2** *The variation of the unit-cell volume with x for $Sn_{1-x}As_xSe$ system (a) and for $SnAs_xSe_{1-x}$ system (b)*

The inset of the Fig. 2a illustrates the XRF map of As of $Sn_{0.95}As_{0.05}Se$ pellet indicating an inhomogeneous embedding of As in the SnSe matrix.

The prepared hot-pressed samples (pellets) showed anisotropic transport properties due to a preferential orientation of the layered SnSe crystallites and the uniaxial pressure of the hot-pressing process. That is why we have measured the transport properties of the pellets in the direction perpendicular to the pressing force. In the Fig. 3, we present electrical conductivity as a function of temperature for both systems studied. The electrical conductivity for the samples of nominal composition $Sn_{1-x}As_xSe$ are presented in the log σ scale (Fig. 3a) for an easier analysis of the variations under observations.

The electrical conductivities σ of the $Sn_{1-x}As_xSe$ samples (Fig. 3a) exhibit a semiconducting behavior and they are increasing with temperature in the whole temperature range. It is evident from Fig. 3a that even a very small addition of As causes a steep decrease in the electrical conductivity. The electrical conductivity further continuously decreases with the increasing nominal content of As in $Sn_{1-x}As_xSe$ samples. Alike, a pronounced decrease of the electrical conductivity is observed upon As-doping also for $SnSe_{0.9985}As_{0.0015}$ system as shown in Fig. 3b. The electrical conductivity of the samples with a higher content of As first increases to 520 K, then switches to metallic-like behavior up to about 650 K and, finally, again increases most likely due to the thermal carrier excitations over the fundamental gap [11].
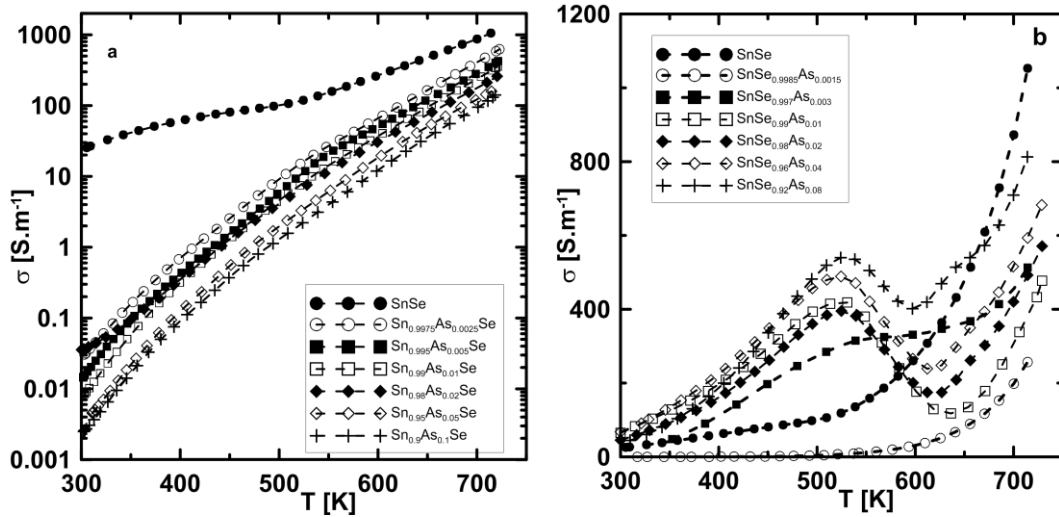
Fig. 3 *Electrical conductivities of Sn$_{1-x}$As$_x$Se samples (a) and SnAs$_x$Se$_{1-x}$ samples (b) as a function of temperature*

The electrical conductivities of Sn$_{1-x}$As$_x$Se samples are plotted in the logarithmic scale for better readability.

Seebeck coefficient S of the undoped SnSe (Fig. 4a,b) is positive and almost temperature independent in the range studied with a small deviation around 520 K. For the Sn$_{1-x}$As$_x$Se samples, even a small substitution of As for Sn causes a steep decrease of S values at lowest temperatures studied. That abrupt decrease with the decreasing temperature (even down to negative values of S for the samples with highest x) indicates that the samples approach an extrinsic regime and, eventually, switch from p-type to n-type. Thus, As-atom behaves like donor (although of very low efficiency), which can be expressed by the equation: $As_{Sn} \rightarrow As_{Sn}^+ + e^-$.
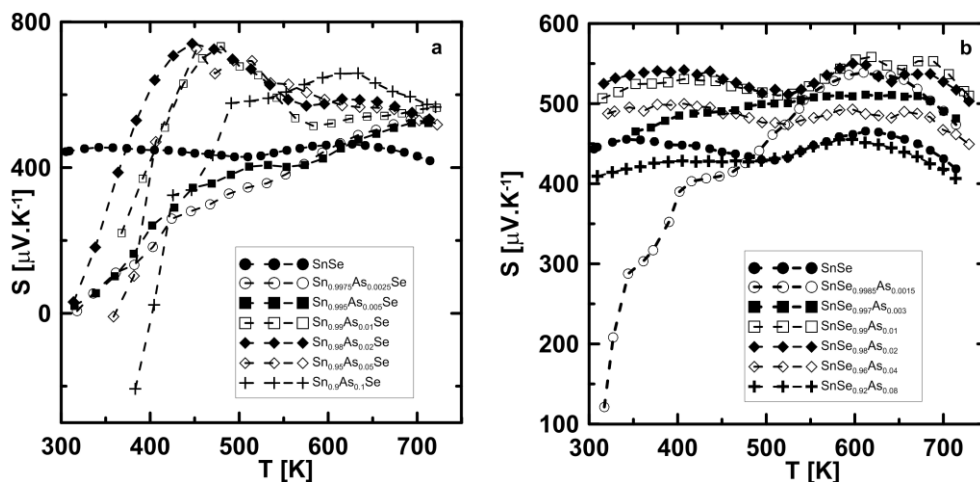

Fig. 4 *Seebeck coefficient of Sn$_{1-x}$As$_x$Se samples (a) and SnAs$_x$Se$_{1-x}$ samples (b) as a function of temperature*

It is not clear whether the As_{Sn} compensates the carriers due to the p-type native defects or its presence in the matrix decreases the concentration of the native defects. We note that this is in accordance with the above presented strong decrease of σ values of these samples with the increasing x. At higher temperatures, values S for all the samples are positive. Similar steep decrease of S is observed also for the lowest values of x in the $SnSe_{1-x}As_x$ system ($SnSe_{0.9985}As_{0.0015}$) at low temperatures. The Seebeck coefficient is positive for the samples of the higher x values and almost temperature-independent, resembling thus the behavior of the undoped SnSe sample (including the irregularity at 520 K).

In the Fig. 5, we present the Arrhenius plot to elucidate the observed variations in the transport properties of some $Sn_{1-x}As_xSe$ samples. In the undoped sample ($x = 0$), the exponential increase of the electrical conductivity at higher temperatures corresponds to a thermal activation of free carriers. It can be characterized by the activation energy of E_a ~0.43 eV, which corresponds to an activation over band gap energy E_g ~0.86 eV. This value is very close to the published values [1,12]. To explain the observed changes in the plot for undoped SnSe, we need to outline a picture of point defects in this compound. As hinted by density functional theory (DFT) and the respective calculations [13–15] together with direct imaging by high-resolution scanning tunneling microscopy (HRSTM) [13,16], the tin vacancies V_{Sn}^{2-} play a dominant role in the electronic properties of the undoped SnSe. This fact is implicitly supported by the formation of metallic Sn in the hot-pressed pellets of some of the samples studied (see Fig. 1). In addition, some of the XRF results indicate a small under-stoichiometry of Sn in our samples. Taking into account this, we can interpret the observed changes viewed in a plot in Fig. 5 as follows. According to the DFT calculations [13–15], the V_{Sn}^{2-} act as a shallow acceptor with a very low activation energy, i.e. it forms acceptors levels very close to the valence band edge. This picture nicely matches the activation energy (0.08 eV) in the extrinsic part of the plot (filling the acceptor levels) followed by the band gap excitation; see Fig. 5a. It presents only two doped samples, one with the lowest x and another one with the highest x. It shows that even a very small addition of As significantly suppresses the electrical conductivity of the compound. In our opinion, the As atoms substituting for Sn effectively prevent the formation of V_{Sn}^{2-} defects. The depletion of the negatively charged vacancies compensated by holes markedly lowers the concentration of the holes and the conductivity decreases. Seebeck coefficient (see Fig. 4a) hints that some positively charged defects compensated by the electrons start to play a major role in the lower temperatures region instead. Regarding the limited solubility of As in $Sn_{1-x}As_xSe$ samples (Fig. 2a), we can offer two explanations. First, a part of the As atoms can substitute for Sn atoms, forming positively charged substitutional As_{Sn}^+ defects compensated by the electrons. Alternatively, the suppression of the V_{Sn}^{2-} defects can reveal the existence of other positively charged point defects, contributing to the electrical transport. These could be

selenium vacancies V_{Se}, which was directly observed in the undoped SnSe [13]. We anticipate a participation of both effects. According to DFT calculations presented in [13], the extra electrons created by V_{Se} seem to be strongly localized near the vacancies sites (i.e. having high activation energy) and they are not expected to significantly contribute to the overall electron transport in the SnSe molecule. However, another DFT calculations have shown [14] that the formation energy of V_{Se} (either V_{Se}^{0} or V_{Se}^{+1}) is relatively low and close to that of V_{Sn}^{2-}, which guarantees rather large concentration of the V_{Se} vacancies.

Here, the authors conclude that the stable neutral state of the vacancies which act as deep donors is the most probable scenario. Such vacancies are, in our opinion, already present even in the undoped sample, but they do not contribute significantly to the total transport dominated by the holes generated by V_{Sn}^{2-}. The strong suppression of the tin vacancies (V_{Sn}^{2-}) due to entering of the As atoms on their sites plays the major role in that the V_{Se} may govern the transport properties. Moreover, the observed activation energies at both low temperatures (~0.35 eV) and higher temperatures (~0.75 eV) nicely corresponds to DFT calculations of the transition energy levels of $V_{Se}(-1/0)$ and $V_{Se}(0/+1)$. Thus, we can explain a large change in the slope of the Arrhenius plots (~0.35 eV *vs.* ~0.75 eV) for $Sn_{1-x}As_{x}Se$ samples ($x \geq 0.0015$) as a change from (originally) trapped to mobile extrinsic electrons with the increasing temperature according to the scheme presented in the inset in Fig. 5a. At the same, we do not exclude some role of the As_{Sn}^{+} substitutional defect that should be compensated by the electrons. The dominant role of the V_{Se} in the electric transport is corroborated by strong resemblance with the $SnSe_{1-x}$ system reported in ref. [17].
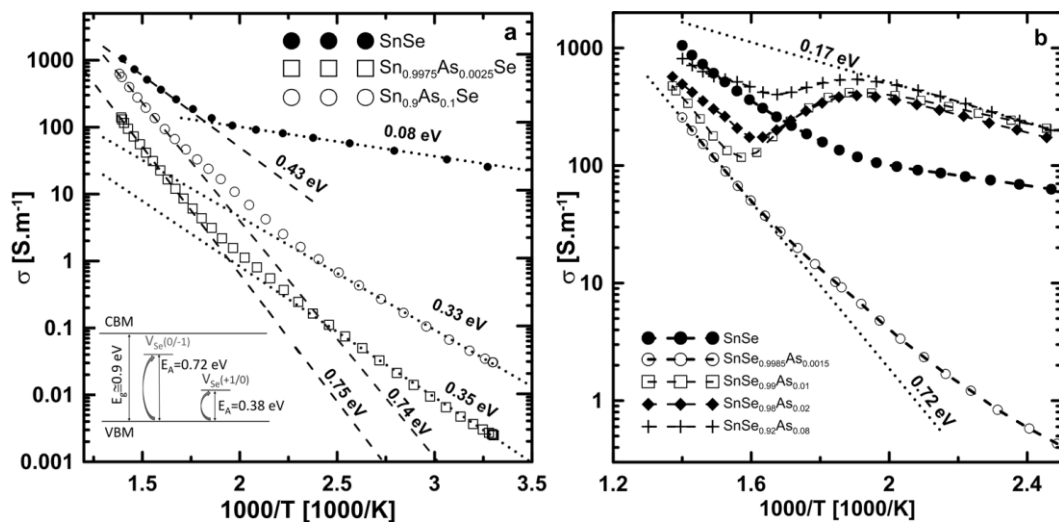

Fig. 5 *Arrhenius plots of the electrical conductivities for selected $Sn_{1-x}As_{x}Se$ samples (a) and $SnAs_{x}Se_{1-x}$ samples (b)*

Activation energies of the present defects calculated from the slopes (dotted lines) are given. Based on [14], suggested energetic scheme of selenium vacancy levels within the band gap of SnSe is presented in the inset of the Fig. 5a.

For the system of nominal composition $SnSe_{1-x}As_x$, one can see again a very pronounced decrease of σ at the sample with the lowest As content, i.e. $SnSe_{0.9985}As_{0.0015}$. A qualitative resemblance of the temperature dependencies of both σ and S for this sample with those observed for the $Sn_{1-x}As_xSe$ leads us to the conclusion that even small substitution of the As atoms for Se atoms strongly suppresses again the formation of major native defects, i.e. tin vacancies V_{Sn}^{2-} in undoped SnSe. However, further increase of nominal composition of As in $SnSe_{1-x}As_x$ samples leads to higher σ-values. The Seebeck coefficient of the samples (see Fig. 4b) with higher x ($x \geq 0.003$) is of p-type character and its nature resembles that of the undoped SnSe sample. The Arrhenius plot (Fig. 5b) reveals an activation energy of 0.17 eV for the samples with $x > 0.01$ in the lower temperature range. Such activation energy could be connected with the formation of As_{Se}^- defects introducing an acceptor level in the band gap of SnSe. This idea is acceptable regarding the variations of the lattice parameters (Fig. 2) and by taking into account the close ionic radii of As^{3-} and Se^{2-} ions (222 ppm *vs.* 198 ppm). A temporary decrease of the electrical conductivity σ at temperatures around 520 K can correspond to a full ionization of the defects, i.e. saturation of the acceptor levels. The following increase of σ at highest studied temperatures is due to the excitations over band gap. Yet another explanation of the observed decrease of electrical conductivities at $T \sim 520$ K and the already mentioned deviation in the Seebeck coefficients at the same temperature can be related to a possible melting of tin as adumbrated in [18]. As follows from the Sn-Se phase diagram [19], there is eutectic point at 504 K (L $\leftrightarrow$ Sn + SnSe) and, as we note above, a small amount of metallic tin is evident in X-ray patterns of the hot-pressed pellets. Moreover, we should consider the presence of other phase in the $SnSe_{1-x}As_x$ compounds studied. As stated above, AsSn impurity was observed in the samples with higher x ($x \geq 0.03$). This compound, classified as NaCl-type superconductor, has electrical conductivity of about 2×10^6 S m^{-1} at room temperature [20]. Taking into account the formation of this compound and the decrease of the lattice parameters (Fig. 2b), we think that a part of the As atoms substitutes for Se atoms, while the remaining As reacts with Sn to form the binary AsSn. One can see, according to simple schematic equation, *$SnSe_{1-x}As_x \leftrightarrow xAsSn + (1-x)\ SnSe$*, that formation of this compound leaves the stoichiometry of the host compound SnSe unaffected. Thus, we can explain the observed variations of σ and S for the samples as follows. A part of As enters the Se-sublattice forming As_{Se}^- and, at very low concentrations ($x \leq 0.003$), this type of defects prevents the formation of tin vacancies as the major defects in the undoped SnSe. With the increased x, the As_{Se}^- defects become the main source of free holes responsible for the increase of electrical conductivity and for restoring the "pure" p-type character of the Seebeck coefficient. After reaching the solubility limit in $SnSe_{1-x}As_x$, As reacts with Sn to form AsSn in $SnSe_{1-x}As_x$ samples.

According to a general effective medium model (GEM) for such composites, the presence of the highly conductive impurity (σ_{300}(AsSn) $\sim 2 \times 10^6$ S m^{-1} [20]) contributes to an additional shift of electrical conductivities towards higher values with the increasing content of As.

Total thermal conductivities κ_{tot} of the studied samples as a function of temperature are presented in Fig. 6a (Sn$_{1-x}$As$_x$Se) and in Fig. 6b (SnSe$_{1-x}$As$_x$). We assume that the total thermal conductivity comprises two contributions in the temperature range studied, i.e. the electronic thermal conductivity κ_{el} and lattice thermal conductivity κ_{lat}. κ_{el} can be estimated by means of Wiedemann-Franz law ($\kappa_{el} = L \times \sigma \times T$, where L is the Lorentz number). However, the electronic contribution to the total thermal conductivity could be considered as negligible even when taking a degenerate limit of the Lorentz number ($L_0 = 2.45 \times 10^{-8}$ W Ω K^{-2}) into account. In the case of Sn$_{1-x}$As$_x$Se system, it acquires its highest value of about 0.5 % from the κ_{tot}, whereas, in the case of SnSe$_{1-x}$As$_x$, it is maximally about 1.5 % of the κ_{tot}. Thus, we consider that the measured thermal conductivity corresponds to its lattice part and it is evident that the thermal conductivity decreases for both systems (Sn$_{1-x}$As$_x$Se and SnSe$_{1-x}$As$_x$) with the increasing x up to $x \leq 0.02$ for Sn$_{1-x}$As$_x$Se and $x \leq 0.01$ for SnSe$_{1-x}$As$_x$. Interestingly, it starts to grow again for higher x. With regard to the XRD results, the increase is probably associated with the formation of the secondary phases in these samples, i.e As in Sn$_{1-x}$As$_x$Se samples and AsSn compound in SnSe$_{1-x}$As$_x$. The presence of highly conductive AsSn adduct causes much higher increase of κ_{tot} than that in the presence of metallic As impurity.
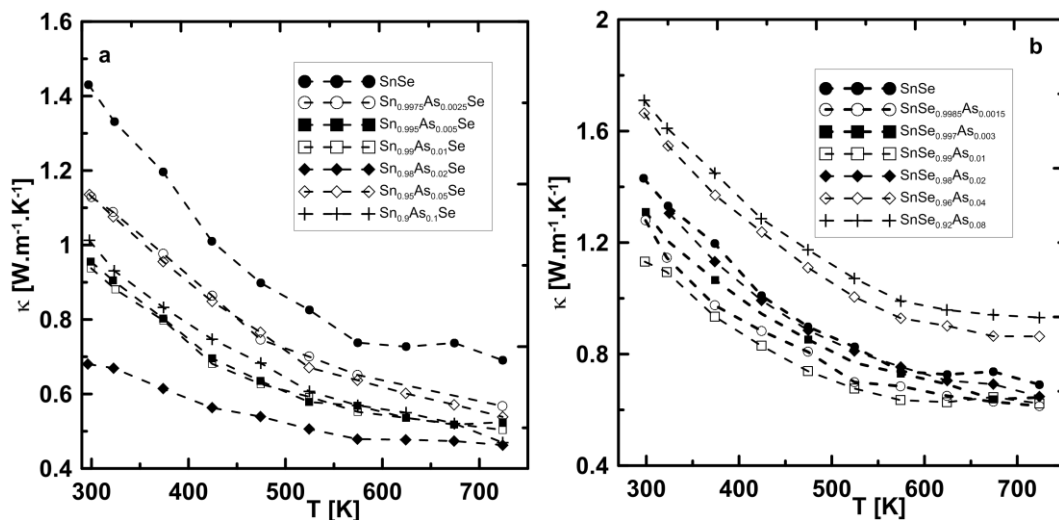

Fig. 6 *Thermal conductivities of Sn$_{1-x}$As$_x$Se samples (a) and SnAs$_x$Se$_{1-x}$ samples (b) as a function of temperature.*

The dimensionless figure of merit *ZT* as a function of *T*, for both systems studied is shown in Fig. 7ab. In the case of Sn$_{1-x}$As$_x$Se (Fig. 7a), one can see that *ZT* values are for all samples lower at low temperatures.

With the increasing temperature, *ZT* values of the samples of lower *x* (0.0025 ≥ *x* ≥ 0.01) either quickly achieve the values for the undoped SnSe or even exceed it (in the samples of nominal composition $Sn_{0.9975}As_{0.0025}Se$). In fact, there are two possible explanations. Such a low concentration of As is very unlikely to change the band structure. More likely, As may facilitate the formation of native defects that are beneficial for thermoelectric properties. Much steeper increase of *ZT* for these samples (compared to undoped sample) would promise an improvement of *ZT* at higher than studied temperatures. However, we note that the chemical stability of doped samples is questionable at elevated temperatures and calls for further explorations. On the other hand, *ZT* values most of the $SnAs_xSe_{1-x}$ samples significantly exceed the one for the undoped SnSe in the temperature range up to *ca.* 520 K, then, it suddenly fall below and being still lower than that of undoped SnSe at higher temperatures. Most likely, it is due to the presence of highly conductive AsSn phase.
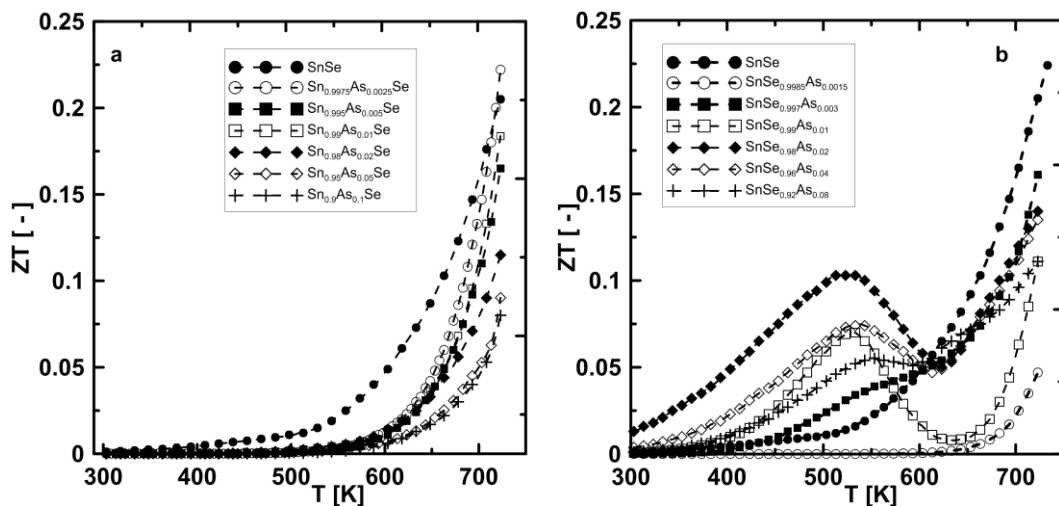

Fig. 7 *Figure of merit ZT of $Sn_{1-x}As_xSe$ samples (a) and $SnAs_xSe_{1-x}$ samples (b) as a function of temperature.*

Conclusions

The effect of the As impurity on the properties of SnSe was studied for doping in both cation sub-lattice and anion sub-lattice. Series of polycrystalline samples with nominal composition $Sn_{1-x}As_xSe$ (0 ≥ *x* ≥ 0.1) and $SnAs_xSe_{1-x}$ (0 ≥ *x* ≥ 0.08) were prepared by melting and hot-pressing. It has been found that in both studied systems, the As-atom very effectively suppresses the formation of the major defect occurring in the undoped SnSe, i.e. the tin vacancy V_{Sn}^{2-}. Apparently, a similar limited solubility of As was found in its substitution at the cation site (*x* ≤ 0.02 for $Sn_{1-x}As_xSe$), as well as the anion site (*x* ≤ 0.03 for $SnAs_xSe_{1-x}$). Here, one can conclude that As behaves as an amphoteric dopant, i.e. substitutes both for the cation (As_{Sn}^+) and the anion (As_{Se}^-), however, neither of the defects does

not significantly contribute to the electronic transport. Moreover, the thermoelectric properties of the studied systems are affected by the formation of the secondary phases in the matrix compound – either as metallic As inclusions or amorphous As-Se phase in the case of $Sn_{1-x}As_xSe$ and AsSn crystalic phase regarding $SnAs_xSe_{1-x}$. Thus, the thermoelectric efficiency is either not enhanced at all (in the case of $Sn_{1-x}As_xSe$) or it is enhanced only in the middle of the temperature range studied (for $SnAs_xSe_{1-x}$).

Acknowledgement

References

[1] Zhao L.D., Lo S.H., Zhang Y.S., Sun H., Tan G.J., Uher C., Wolverton C., Dravid V.P., Kanatzidis M.G.: Ultralow thermal conductivity and high thermoelectric figure of merit in SnSe crystals. *Nature* **508** (2014) 373–377.

[2] Chen C.L., Wang H., Chen Y.Y., Day T., Snyder G.J.: Thermoelectric properties of p-type polycrystalline SnSe doped with Ag. *Journal of Materials Chemistry A* **2** (2014) 11171–11176.

[3] Singh N.K., Bathula S., Gahtori B., Tyagi K., Haranath D., Dhar A.: The effect of doping on thermoelectric performance of p-type SnSe: Promising thermoelectric material. *Journal of Alloys and Compounds* **668** (2016) 152–158.

[4] Chen Y.X., Ge Z.H., Yin M.J., Feng D., Huang X.Q., Zhao W.Y., He J.Q.: Understanding of the extremely low thermal conductivity in high-performance polycrystalline SnSe through potassium doping. *Advanced Functional Materials* **26** (2016) 6836–6845.

[5] Leng H.Q., Zhou M., Zhao J., Han Y.M., Li L.F.: The thermoelectric performance of anisotropic SnSe doped with Na. *RSC Advances* **6** (2016) 9112–9116.

[6] Ge Z.H., Song D.S., Chong X.Y., Zheng F.S., Jin L., Qian X., Zheng L., Dunin-Borkowski R.E., Qin P., Feng J., Zhao L.D.: Boosting the Thermoelectric Performance of (Na,K)-Codoped Polycrystalline SnSe by Synergistic Tailoring of the Band Structure and Atomic-Scale Defect Phonon Scattering. *Journal of the American Chemical Society* **139** (2017) 9714–9720.

[7] Li D., Li J.C., Qin X.Y., Zhang J., Xin H.X., Song C.J., Wang L.: Enhanced thermoelectric performance in SnSe based composites with PbTe nanoinclusions. *Energy* **116** (2016) 861–866.

[8] Sassi S., Candolfi C., Vaney J.B., Ohorodniichuk V., Masschelein P., Dauscher A., Lenoir B.: Assessment of the thermoelectric performance of polycrystalline p-type SnSe. *Applied Physics Letters* **104** (2014) 212105-1–212105-4.

[9]   Shannon R.D.: Revised effective ionic-radii and systematic studies of interatomic distances in halides and chalcogenides. *Acta Crystallographica Section A* **32** (1976) 751–767.

[10]   Wei W., Chang C., Yang T., Liu J., Tang H., Zhang J., Li Y., Xu F., Zhang Z., Li J.-F., Tang G.: Achieving high thermoelectric figure of merit in polycrystalline SnSe via introducing Sn vacancies. *Journal of the American Chemical Society* **140** (2018) 499–505.

[11]   Tang G.D., Wei W., Zhang J., Li Y.S., Wang X., Xu G.Z., Chang C., Wang Z.H., Du Y.W., Zhao L.D.: Realizing high figure of merit in phase-separated polycrystalline $Sn_{1-x}Pb_xSe$. *Journal of the American Chemical Society* **138** (2016) 13647–13654.

[12]   Yu J.G., Yue A.S., Stafsudd O.M.: Growth and electronic properties of the SnSe semiconductor. *Journal of Crystal Growth* **54** (1981) 248–252.

[13]   Duvjir G., Min T., Ly T.T., Kim T., Duong A.T., Cho S., Rhim S.H., Lee J., Kim J.: Origin of p-type characteristics in a SnSe single crystal. *Applied Physics Letters* **110** (2017).

[14]   Huang Y.C., Wang C., Chen X., Zhou D.M., Du J.Y., Wang S.F., Ning L.X.: First-principles study on intrinsic defects of SnSe. *RSC Advances* **7** (2017) 27612–27618.

[15]   Dewandre A., Hellman O., Bhattacharya S., Romero A.H., Madsen G.K.H., Verstraete M.J.: Two-step phase transition in SnSe and the origins of its high power factor from first principles. *Physical Review Letters* **117** (2016).

[16]   Wu D., Wu L.J., He D.S., Zhao L.D., Li W., Wu M.H., Jin M., Xu J.T., Jiang J., Huang L., Zhu Y.M., Kanatzidis M.G., He J.Q.: Direct observation of vast off-stoichiometric defects in single crystalline SnSe. *Nano Energy* **35** (2017) 321–330.

[17]   Lv S., Ge Z.H., Chen Y.X., Zhao K.Y., Feng J., He J.Q.: Thermoelectric properties of polycrystalline SnSe1 +/− x prepared by mechanical alloying and spark plasma sintering. *RSC Advances* **6** (2016) 92335–92340.

[18]   Lee S.T., Kim M.J., Lee G.G., Kim S.G., Lee S., Seo W.S., Lim Y.S.: Effects of Sn-deficiency on thermoelectric properties of polycrystalline $Sn_{1-x}Se$ compounds. *Current Applied Physics* **17** (2017) 732–737.

[19]   Sharma R.C., Chang Y.A.: The Se−Sn (Selenium–Tin) system. *Bulletin of Alloy Phase Diagrams* **7** (1986) 68–72.

[20]   Wang Y., Sato H., Toda Y., Ueda S., Hiramatsu H., Hosono H.: SnAs with the NaCI-type structure. Type-I: Superconductivity and single valence state of Sn. *Chemistry of Materials* **26** (2014) 7209–7213.